Time-frequency representation of Lamb waves using the reassigned spectrogram

Marc Niethammer, Laurence J. Jacobs

School of Civil and Environmental Engineering,
Georgia Institute of Technology, Atlanta, Georgia 30332-0355
mn@kyb.uni-stuttgart.de; laurence.jacobs@ce.gatech.edu

Jianmin Qu, Jacek Jarzynski

G.W. Woodruff School of Mechanical Engineering,
Georgia Institute of Technology, Atlanta, Georgia 30332-0405
jianmin.qu@me.gatech.edu; jacek.jarzynski@me.gatech.edu

Abstract: This brief note reports on a study that applies the reassigned spectrogram (the reassigned energy density spectrum of the short-time Fourier transform [STFT]) to develop the dispersion curves for multimode Lamb waves propagating in an aluminum plate. The proposed procedure first uses the spectrogram to operate on a *single*, laser-generated and detected waveform to develop the dispersion relationship for this plate. Next, a reassignment procedure is used to refine the time-frequency resolution of the calculated dispersion curves. This reassignment operation clarifies the definition of the measured modes. This study demonstrates that the reassigned spectrogram is capable of distinguishing multiple, closely spaced Lamb modes in the ultrasonic frequency range.

PACS number: 43.20.Mv, 43.35.Cg

1. Introduction

This research demonstrates the effectiveness of using the reassigned spectrogram to characterize laser-generated and detected Lamb waves. By applying the reassigned spectrogram to an ultrasonic waveform measured in a flat aluminum plate, it is possible to accurately determine the dispersion relationship for this plate.

Lamb waves, which are dispersive and contain multiple modes, have received extensive attention since the study by Mindlin.[1] Recent experimental work has shown that it is possible to obtain a plate's dispersion relationship by using the two-dimensional Fourier transform (2D-FT) to operate on multiple, equally spaced waveforms.[2,3] Unfortunately, the need for exact, spatially sampled data restricts the practicality of the 2D-FT for some inspection applications. In contrast, time-frequency representations (TFRs) require only a single signal. Recently, Prosser *et al.*[4] used the smoothed Wigner-Ville distribution (a TFR) to determine the Lamb modes of numerically simulated waveforms in an aluminum plate. They also consider real experimental data for a composite plate and identify the s_0 and the a_0 Lamb modes for frequencies below 500 kHz. Hayashi *et al.*[5] determined the thickness and the elastic properties of thin metallic foils (thickness of less than $40\ \mu m$) by calculating the group velocity of a single mode (the a_0 up to 3.5 MHz) using the wavelet transform (another TFR) of laser-generated and detected Lamb waves.

The current study shows that the reassigned spectrogram is an extremely accurate TFR capable of distinguishing multiple (seven in this example), closely spaced Lamb modes in the ultrasonic frequency range (up to 10 MHz).

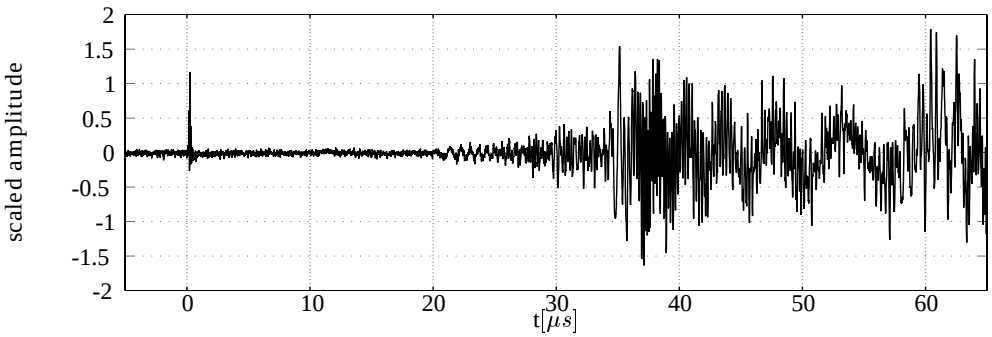

Fig. 1: Time-domain signal measured in 0.93 mm aluminum plate, propagation distance of 11 cm.

2. Transient time-domain signal

The experimental procedure makes high-fidelity (resonance-free) measurements of Lamb waves over a wide frequency range (200 kHz to 10 MHz). Broad-bandwidth Lamb waves are generated with the beam from a Nd:YAG laser (4-6 ns pulse) (see Scruby and Drain[6] for details on laser ultrasonics). Laser detection of these waves is accomplished with a heterodyne interferometer[7] that uses the Doppler shift to measure out-of-plane surface velocity (particle velocity) at a point on the specimen's surface. The high-fidelity, broad-bandwidth and noncontact nature of laser ultrasonics are critical elements for the success of this research. The specific plate examined is 0.93 mm thick 3003 aluminum, 203 mm long by 153 mm wide.

Figure 1 shows a (transient) time-domain signal with a propagation distance of 11 cm measured in the 0.93 mm aluminum plate. The Nd:YAG laser fires at $t = 0$ and generates a Lamb wave at the source location (the spot where the Nd:YAG hits the plate). Note that the electromagnetic discharge of the Nd:YAG's firing causes a spurious noise spike at $t = 0$. The signal in Fig. 1 is discretized with a sampling frequency of 100 MHz, low-passed filtered at 10 MHz, and represents an average of one hundred Nd:YAG shots to increase the signal-to-noise ratio.

3. The reassigned spectrogram — background

It is possible to use a TFR to transform this signal (Fig. 1) into the time-frequency domain and then quantitatively characterize the plate's features. This study establishes the effectiveness of using a specific TFR, the reassigned spectrogram, to accomplish this task. Instead of considering the Fourier transform of the entire signal at once, use the STFT to chop a signal into a series of small overlapping pieces. Each of these pieces is windowed and then individually Fourier transformed.[8] The STFT of a function $s(t)$ is defined as:

$$S(\omega, t) = \frac{1}{2\pi} \int_{-\infty}^{\infty} e^{-i\omega\tau} s(\tau) h(\tau - t) \mathrm{d}\tau, \tag{1}$$

where $h(t)$ is a window function. The energy density spectrum of a STFT is defined as $E(\omega, t) = |S(\omega, t)|^2$ and called a spectrogram.

Unfortunately, TFRs such as the spectrogram suffer from the Heisenberg uncertainty principle,[8] making it impossible to simultaneously have perfect resolution in both time and frequency. The standard deviations for time and frequency, σ_t and σ_ω,

respectively, of the window function for a specific spectrogram are not independent of each other; the Heisenberg uncertainty principle limits a spectrogram's time and frequency resolution by the following inequality:[9] $\sigma_t^2\sigma_\omega^2 \geq 0.25$. Note that the window type ($h(t)$) determines the time-frequency spread of a spectrogram.[9] For example, the product of $\sigma_t^2\sigma_\omega^2$ is 0.2635 for a spectrogram calculated with a Hanning window. A Gaussian window function satisfies the equality $\sigma_t^2\sigma_\omega^2 = 0.25$, but the current application aims to alter the shape of the time signal as little as possible while avoiding discontinuities across the boundaries of the windowed signal.[9] The Hanning window is chosen as a compromise.

The time-frequency resolution of a spectrogram depends only on the window size and type and is independent of frequency. A wide window gives better frequency resolution, but worsens the time resolution, whereas a narrow window improves time resolution but worsens frequency resolution. This is in contrast to a wavelet transform;[9] the wavelet transform tiles the time-frequency plane in an irregular fashion, resulting in a frequency dependent, time-frequency resolution. The wavelet transform of small frequency values provides good frequency resolution, but the time resolution is bad. On the other hand, the wavelet transform of large frequency values provides poor frequency resolution, but the time resolution is good.

It is possible to improve the time-frequency resolution of a spectrogram with the reassignment method, a technique developed by Auger and Flandrin[11] that provides a computationally efficient way to compute the modified moving window method first proposed by Kodera *et al.*[12] for the spectrogram and the scalogram (the energy density spectrum of a wavelet transform). In the reassignment method, "energy" is moved away from its original location, coordinates (t,ω), to a new location, the reassigned coordinates $(\hat{t},\hat{\omega})$, thus greatly reducing the "spread" of a spectrogram. The reassignment method improves the time-frequency resolution of a spectrogram by concentrating its energy at a center of gravity. Note that the reassignment method is not restricted to a specific TFR such as the spectrogram but can be applied to any time-frequency shift invariant distribution of Cohen's class.[8]

Auger and Flandrin[11] show that the reassigned coordinates $\hat{t}$ and $\hat{\omega}$ for a spectrogram are:

$$\hat{t} = t - \Re\left(\frac{S_{\mathcal{T}h}(x,t,\omega)\cdot\overline{S_h(x,t,\omega)}}{|S_h(x,t,\omega)|^2}\right) \tag{2}$$

and:

$$\hat{\omega} = \omega - \Im\left(\frac{S_{\mathcal{D}h}(x,t,\omega)\cdot\overline{S_h(x,t,\omega)}}{|S_h(x,t,\omega)|^2}\right) \tag{3}$$

where $S_h(x,t,\omega)$ is the STFT (Eq. 1) of the signal x using a normalized window function $h(t)$; and $S_{\mathcal{T}h}(x,t,\omega)$ and $S_{\mathcal{D}h}(x,t,\omega)$ are the STFT's with $t\cdot h(t)$ and $\frac{\mathrm{d}h(t)}{\mathrm{d}t}$ as their respective window functions. The application of Eqs. 2 and 3 is computationally straight forward and implemented with a MATLAB program.

4. The reassigned spectrogram — application to Lamb waves

Assessment of the the accuracy of the dispersion curves obtained with the spectrogram and the reassigned spectrogram requires benchmark, analytical results, obtained by solving the Rayleigh-Lamb frequency spectrum.[1] Solution of the Rayleigh-Lamb spectrum provides dispersion curves in the frequency-wavenumber (f,k) domain, whereas

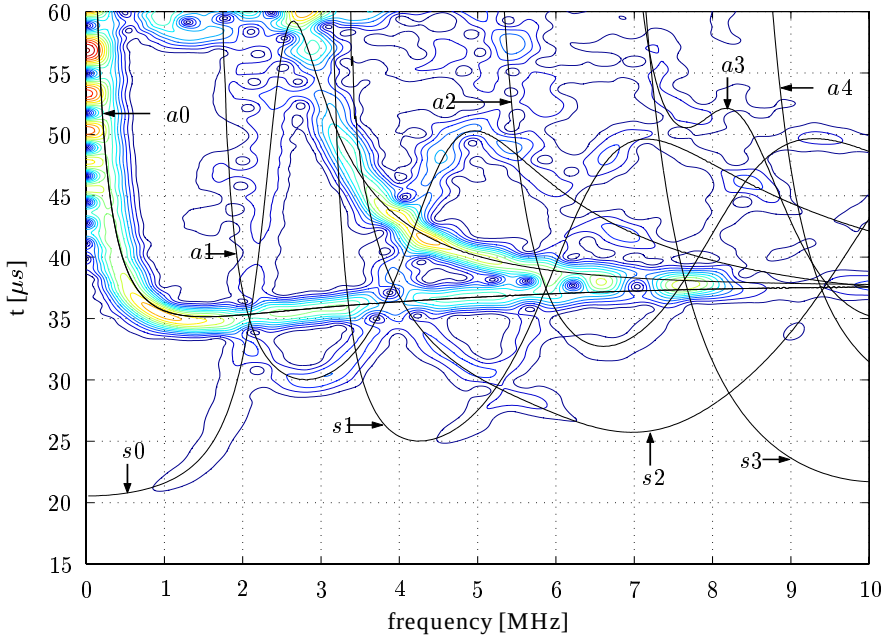

Fig. 2: "Original" spectrogram of the time-domain signal in Fig. 1 obtained with a 384-point Hanning window plus analytical modes (solid lines). Note that Figs. 2 through 4 appear in color in the archived online version of this brief note.

the spectrogram maps a signal into the time-frequency domain. To obtain the analytical dispersion curves in the time-frequency domain, the group velocities for each of the different modes at all relevant frequencies are determined by numerically differentiating f with respect to k.

Fig. 2 shows a contour plot of the square root of a spectrogram of the signal in Fig. 1 for a 384-point long Hanning window together with the analytically obtained dispersion curves (solid lines). The (experimental) s_0 and a_0 modes are clearly visible through the entire frequency bandwidth (to 10 MHz), the a_1 mode appears from 2 MHz to 7 MHz, and traces of the s_1, s_2 and a_2 modes are evident. Overall, there is very good agreement between the analytical and experimental results, although there is a general lack of time-frequency resolution (clarity) in the experimental results. For example, it is difficult to positively identify the individual modes for frequencies above 5 MHz and times greater than $40\ \mu s$. Note that Niethammer[10] calculates spectrograms for a variety of Hanning window lengths for the signal shown in Fig. 1 and determines that the 384-point window provides the best compromise between time and frequency resolution for this multimode, ultrasonic signal.

The reassignment method is used to improve the time-frequency resolution of this "original" spectrogram, providing better clarity and definition of the individual modes. Fig. 3 shows a contour plot of the square root of the reassigned spectrogram obtained by applying the reassignment procedure (Eqs. 2 and 3) to the original spectrogram of Fig. 2. The reassigned spectrogram (Fig. 3) provides a crisper definition of the individual modes (when compared to the original spectrogram), and the reassigned, experimental modes are localized to the analytical curves. However, some lack of definition occurs at the intersection of modes. These "fuzzy" regions illustrate one difficulty with the reassignment method — the strongest mode (the one with the high-

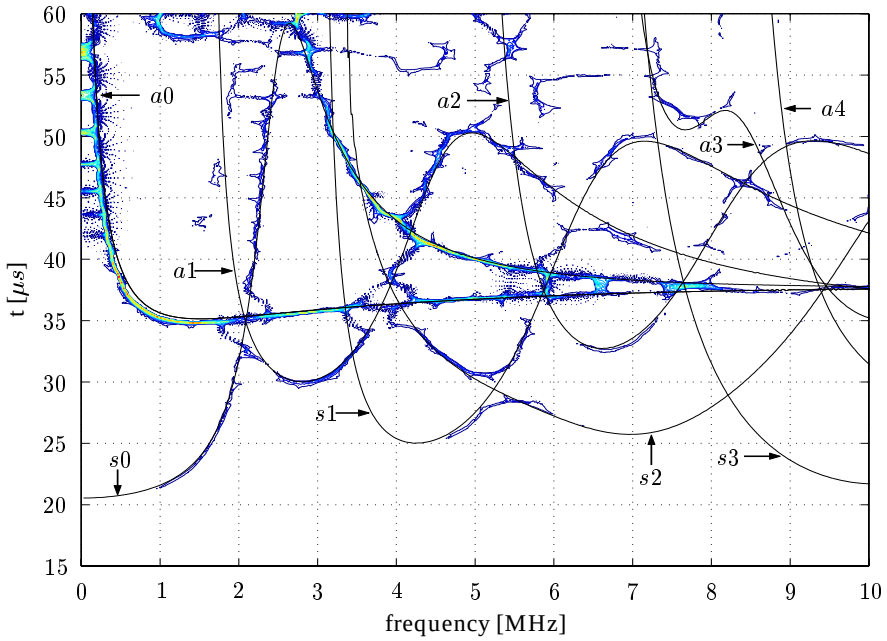

Fig. 3: Reassigned spectrogram obtained by reassignment of the original spectrogram in Fig. 2.

est amplitude in the spectrogram) becomes the mode that attracts the center of gravity during reassignment. As a result, the strongest mode remains a continuous line, but this continuity is at the expense of weaker modes that become separated in the intersection region (e.g., the intersection of the a_0 and s_0 modes around 2 MHz in Fig. 3). Finally, broken lines show up above $50\ \mu s$. These are most likely caused by reflections from the boundaries of the plate and can sometimes (especially for short propagation distances to the boundaries) lead to unwanted distortion of the reassigned spectrogram. Overall, there is excellent definition of seven modes (s_0–s_2 and a_0–a_3) through a wide frequency range (up to 10 MHz), demonstrating that the reassigned spectrogram is capable of distinguishing multiple, closely spaced Lamb modes in the ultrasonic frequency range.

An additional portion of this research[10] shows that the wavelet transform is ineffective in resolving the multiple Lamb modes of this aluminum plate through such a wide frequency range. Figure 4 shows the square root of an "original" and reassigned scalogram of the same time-domain signal (Fig. 1) calculated with a Gabor wavelet. Although the time resolution at high frequencies is very good, there is not enough frequency resolution to separate the different modes at the high frequencies (e.g., above 2 MHz). Note that the scalogram is effective in resolving the a_0 mode up to 10 MHz — an important feature for some applications. In addition, the proposed reassignment procedure does not significantly improve the time-resolution of the "original" scalogram in this example.

5. Conclusion

This note clearly demonstrates the effectiveness of applying the reassigned spectrogram to determine the dispersion curves of multi-mode Lamb waves in the ultrasonic

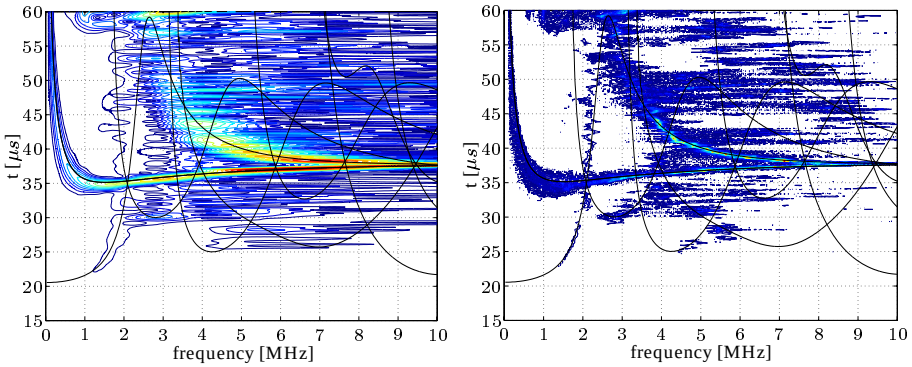

(a) "Original" scalogram (b) Reassigned scalogram

Fig. 4: Scalograms of the time-domain signal in Fig. 1, calculated using a Gabor wavelet.

frequency range, propagating in a flat plate. In general, the "original" spectrogram provides a qualitative representation of the plate's dispersion relationship, whereas the reassignment procedure refines the time-frequency resolution of these dispersion curves. Although the reassigned spectrogram has slight difficulties with mode intersections, this technique is extremely effective in localizing multiple, closely spaced modes in both time and frequency.

Acknowledgment

This work is supported by the Office of Naval Research M-URI Program "Integrated Diagnostics" (Contract number: N00014-95-1-0539). The Deutscher Akademischer Austausch Dienst (DAAD) provided partial support to Marc Niethammer. The authors thank Mr. Christoph Eisenhardt for his contributions.

References

[1] R.D. Mindlin, "Waves and vibrations in isotropic elastic plates," in *Structural Mechanics*, edited by J.N. Goodier and N.J. Hoff (Pergamon Press, New York, 1960).
[2] D. Alleyne and P. Cawley, "A two-dimensional Fourier transform method for measurement of propagating multimode signals," J. Acoust. Soc. Am., **89**, 1159–1168 (1991).
[3] C. Eisenhardt, L.J. Jacobs, and J. Qu, "Application of laser ultrasonics to develop dispersion curves for elastic plates," J. Appl. Mech., **66**, 1043–1045 (1999).
[4] W.H. Prosser, M.D. Seale, and B.T. Smith, "Time-frequency analysis of the dispersion of Lamb modes," J. Acoust. Soc. Am., **105**, 2669–2676 (1999).
[5] Y. Hayashi, S. Ogawa, H. Cho, and M. Takemoto, "Non-contact estimation of thickness and elastic properties of metallic foils by wavelet transform of laser-generated Lamb waves," NDT & E Int., **32**, 21–27 (1999).
[6] C. B. Scruby and L.E. Drain, *Laser Ultrasonics: Techniques and Applications* (Adam Hilger, Bristol, 1990).
[7] D.A. Bruttomesso, L.J. Jacobs, and R.D. Costley, "Development of an interferometer for acoustic emission testing," J. Eng. Mech., **119**, 2303–2316 (1993).
[8] L. Cohen, *Time-Frequency Analysis* (Prentice-Hall, New Jersey, 1995).
[9] S. Mallat, *A Wavelet Tour of Signal Processing* (Academic Press, New York, 1998).
[10] M. Niethammer, *Application of Time-Frequency Representations to Characterize Ultrasonic Signals* (M.S. thesis, Georgia Institute of Technology, Atlanta, 1999).
[11] F. Auger and P. Flandrin, "Improving the readability of time-frequency and time-scale representations by the reassignment method," IEEE Trans. Signal Processing **43**, 1068–1089 (1995).
[12] K. Kodera, R. Gendrin and C. de Villedary, "Analysis of time-varying signals with small BT values," IEEE Trans. Acoust., Speech and Signal Processing **26**, 64–76 (1978).